

TransLoc3D : Point Cloud based Large-scale Place Recognition using Adaptive Receptive Fields

Tian-Xing Xu¹, Yuan-Chen Guo¹, Yu-Kun Lai² and Song-Hai Zhang¹

¹BNRist, Department of Computer Science and Technology, Tsinghua University, Beijing

²School of Computer Science & Informatics, Cardiff University

{xtx17, guoyc19}@mails.tsinghua.edu.cn, shz@tsinghua.edu.cn, LaiY4@cardiff.ac.uk

Abstract

Place recognition plays an essential role in the field of autonomous driving and robot navigation. Although a number of point cloud based methods have been proposed and achieved promising results, few of them take the size difference of objects into consideration. For small objects like pedestrians and vehicles, large receptive fields will capture unrelated information, while small receptive fields would fail to encode complete geometric information for large objects such as buildings. We argue that fixed receptive fields are not well suited for place recognition, and propose a novel Adaptive Receptive Field Module (ARFM), which can adaptively adjust the size of the receptive field based on the input point cloud. We also present a novel network architecture, named TransLoc3D, to obtain discriminative global descriptors of point clouds for the place recognition task. TransLoc3D consists of a 3D sparse convolutional module, an ARFM module, an external transformer network which aims to capture long range dependency and a NetVLAD layer. Experiments show that our method outperforms prior state-of-the-art results, with an improvement of 1.1% on average recall@1 on the Oxford RobotCar dataset, and 0.8% on the B.D. dataset.

1. Introduction

Navigation systems are highly demanded for robustly localizing robots and self-driving cars in complex outdoor scenes. Global Positioning System (GPS) is a common solution, which is based on ultra-long range wireless transmission. One kind of alternative methods is to sense the surroundings of agents by LiDARs or RGB cameras and perform localization utilizing these data. Early methods [21, 23, 24] mainly rely on images and have achieved inspiring results. However, compared with point clouds

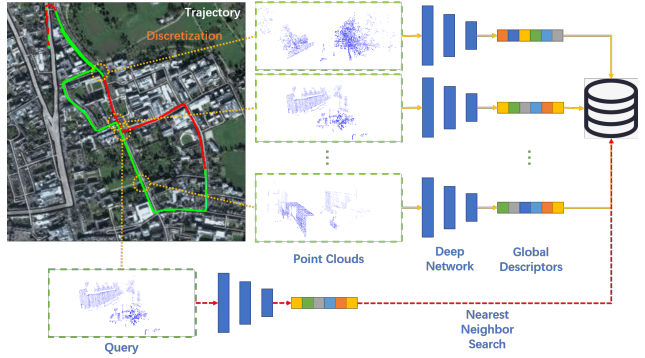


Figure 1. Place recognition pipeline. The continuous trajectories are discretized into places stored with their corresponding point clouds. Our TransLoc3D takes point clouds as input and produces discriminative descriptors for instance retrieval.

from LiDAR sensors, images from RGB cameras are more sensitive to change of illumination caused by different environments, which may lead to significant performance degradation under certain circumstances [46]. To alleviate this problem, more and more works [46, 55, 41, 27, 18, 57] began to focus on 3D point cloud based place recognition due to the inherent invariance of point clouds.

Large-scale point cloud based place recognition is usually seen as an instance retrieval problem. As illustrated in Fig. 1, the trajectories of robot cars are discretized into a series of places. Point clouds scanned from different places (“Point Clouds” in the middle of the figure) are transformed to high-level feature representations (“Global Descriptors” in the middle right) and stored in a large-scale database (right). Given a query point cloud (“Query” at the bottom left), the purpose is to find the closest match from the pre-built database and return its corresponding place. Existing methods can be roughly categorized into two main streams according to the data representations - point cloud based

methods [46, 55, 53, 27, 41, 57] and sparse voxel based methods [18, 19]. PointNetVLAD [46] is the pioneer of point-based methods. In this method, PointNet [35] is firstly adopted to aggregate local information. Then, a NetVLAD layer [1] is used to transform the local descriptors to a global descriptor. However, place recognition relies more on local features, which is not suitable to apply the PointNet architecture directly. LPD-Net[27] and NDT-Transformer[57] have achieved the state-of-the-art results under the time-consuming data preprocessing steps. The former requires precomputing handcrafted local features for each point, and the latter transforms raw coordinates of point clouds to Normal Distribution Transform representation[29]. An alternative to processing unordered point set is to perform sparse voxelization, which is proposed and proved to be effective in MinkLoc3D[18] and MinkLoc++ [19]. They propose to use a sparse convolutional neural network built on Feature Pyramid Network [22] to extract local descriptors. However, these two streams of methods ignore the huge difference in sizes of various objects in complex outdoor scenes. For example, pedestrians and cars are much smaller than buildings. On one hand, oversized receptive field captures unrelated information for small objects, which may affect the understanding of the scene. On the other hand, insufficient receptive field fails to capture entire semantic information. We argue it could result in performance degradation in place recognition.

Inspired by the success of SK-Net[20] for visual tasks, we propose a novel architecture named TransLoc3D for place recognition, which is able to handle size difference in complex outdoor scenes without complex data preprocessing. We first adopt a shallow 3D sparse convolutional neural network to aggregate local information and produce features for each point. It has been proved effective by existing methods [18, 19]. The self-attention[47] mechanism is adopted to capture long-range dependency among local features. The NetVLAD layer[1] takes local descriptors as inputs and outputs a global descriptor. We design a novel Adaptive Receptive Field Module (ARFM) to accurately capture geometric structure of objects in different sizes and incorporate this module into TransLoc3D. With the help of ARFM, TransLoc3D surpasses previous transformer-based method, NDT-Transformer[57], by nearly 1 p.p. on average recall@1 and outperforms the state-of-the-art method.

Our contributions can be briefly summarized as follow

- We analyse the current pipeline of place recognition and argue that different receptive field is necessary in complex scenes recognition. Based on the analysis, we propose a novel Adaptive Receptive Field Module (ARFM) to address this problem.
- We propose a novel architecture named TransLoc3D. It combines the advantages of sparse voxelization, adap-

tive receptive field and transformer, which enables it is suitable for place recognition.

- Extensive experiments demonstrate that the proposed TransLoc3D achieves the state-of-the-art performance on four popular benchmarks Oxford RobotCar dataset, B.D. dataset, U.S. dataset and R.A. dataset.

2. Related work

3D point cloud based place recognition. Before the deep learning-based methods, producing a discriminative global descriptor from a point cloud often relied on hand-crafted local feature extraction, such as [13, 17, 6]. In recent years, the breakthrough of hardware and accumulation of data have greatly promoted the development of learning-based feature extraction methods[35, 36, 15, 54, 50]. From the PointNet[35], learning-based architecture can operate on the raw point cloud data directly. It adopts multi-layer perceptrons to each point to extract independent features, and then aggregate independent features using a symmetric global max pool function making the global descriptors own permutation invariance.

PointNetVLAD[46] is the first learning-based method used for large-scale place recognition, following the design of PointNet[35]. This method adopts NetVLAD[1], an architecture that has achieved great success in image retrieval task, to transform independent features into a global discriminative descriptor. Though PointNet has proven to be promising in point cloud classification, it is not well suitable for PointNet-based architecture to capture local geometric structure. After this, PCAN [55] proposes a Point Contextual Attention module, which can predict the significance of each independent point feature based on point context, to improve the performance of NetVLAD[1] layer in PointNetVLAD[46], while it also ignores the spatial distribution of local area. LPD-Net [27] enhances the input point clouds by introducing ten handcrafted features related to local geometric structure, including change of curvature, omni-variance and so on. Inspired by the success of graph neural network [2], it proposed a graph-based aggregation module in both Feature space and Cartesian space to capture local geometry. Previously mentioned works all operate directly on raw 3D point clouds, and MinkLoc3D[18] uses an alternative data representation for place recognition. Point clouds are discretized into sparse voxelized representation, and then a 3D sparse CNN based on a Feature Pyramid Network[22] is adopted to extract informative local features. Instead of a NetVLAD[1] layer, MinkLoc3D uses a Generalized-Mean pooling layer[37] to produce a global descriptor, which eases the training process efficiently and reduces the number of model parameters. The following work Minkloc++[19] introduces ECA module[48] into Minkloc3D and yields state-of-the-art results.

Transformers in computer vision. Recently, inspired by the success of Vision Transformer[8], more and more researchers focus their attention on applying the Transformer architecture to image classification[12, 49], object detection [7, 42, 3], segmentation [51, 9, 56] and so on. Transformer [47] is a novel self-attention layer-based model used to draw global dependencies between features at various locations in space, which has dominated natural language processing. NDT-Transformer [57] is the first deep learning architecture modelled upon a standard Transformer for place recognition. 3D points are required to be transformed into Normal Distribution Transform Cell (NDT Cell) representation [29] first, and then fed to a transformer with 3 encoders to aggregate information. Following previous work, NDT-Transformer uses a NetVLAD [1] layer to produce a global descriptor. The standard Transformer architecture enable each neurons to have a global receptive field but it suffers from a high cost in complexity and memory, which limits the number of attention layers and leads to poor performance. We propose an alternative to build our transformer with external attention[11], a lightweight attention mechanism with linear computing complexity. Therefore, we can build deeper Transformer-based model to produce more discriminative global descriptors from complex scenes.

Multi-scale receptive fields. Experiments [33, 34, 40] in neuroscience indicate that the receptive field size of a neuron is modulated by bioelectric signal rather than fixed. However, this property does not get the right attention in constructing convolutional neural networks. Previous work [22, 38, 25] mostly aggregate multi-scale features by fusing the outputs of different layers. As far as we know, InceptionNetV1[44] is the first architecture aggregating multi-scale information within the same layer. A simple concatenation mechanism is designed to fusing the outputs from convolutional layers with various kernel sizes. The following work SKNet[20] enhances this architecture using an attention mechanism to fuse multi-scale information from different receptive fields in 2D images. Compared with 1×1 convolutional kernels used in Inception-Nets [44, 45, 43], the attention mechanism is more suited to adaptively adjust the receptive field sizes. Inspired by SKNet[20], we propose a similar module, named Adaptive Receptive Field Module, to tackle the size difference among various objects in out-door scenes.

3. Method

This paper addresses place recognition as an instance retrieval problem for point clouds, and the goal of the proposed architecture is to project point clouds from a high dimensional data space to a low dimensional feature space enriched with semantic and geometric information. The network architecture of our proposed TransLoc3D are shown in Fig. 2. TransLoc3D consists of four main parts, including

Layer	Parameters
Conv0	$\mathbb{C}_{5_k 1_s}^{64}$
Conv1	$\mathbb{C}_{2_k 2_s}^{64}$

Table 1. Details of 3D sparse convolution module. Each convolution is followed by batch normalization and ReLU function.

a 3D sparse convolution module, an adaptive receptive field module, an external transformer and a NetVLAD [1] module. This section describes the design of the above modules first, and then briefly introduces our training process with triplet margin loss [14].

3.1. 3D Sparse Convolution Module

In contrast to single-object 3D models, outdoor scenes have more complex geometric structures. Therefore, the point cloud of a scene often contains several times more points than a single-object model. Point clouds of objects contain 1024 points in ModelNet40[52] dataset for the classification task, while all point clouds are downsampled to have 4096 points in Oxford RobotCar dataset[28]. Most existing methods [35, 36, 26] operating on raw point clouds require computing the Euclidean distance between each two points, because the neighborhood of a point is defined as a spherical area with radius r . The time and space complexity of this step is $O(N^2)$, where N denotes the number of points. Consequently, with the same batch size, a point cloud in Oxford RobotCar dataset consumes 16 times more memory than that in ModelNet40. What’s worse, the number of active triplets (triplets with non-zero loss) obtained by hard negative mining [30] has positive correlation with the batch size. In the late stage of training, a large batch size is required to obtain relatively large number of active triplets so as to improve the performance of proposed model, which also burdens memory consumption.

The success of Minkloc3D [18] shows the protential of sparse voxelization and 3D sparse convolution in the place recognition task. The most prominent advantage of sparse voxel representation is that the neighborhood of each point can be obtained without any additional effort using hashing algorithms. However, it is undeniable that information loss is introduced after discretization. In order to quantify the information loss, we conduct an experiment on how the number of points changes in the process. As shown in Fig. 3, about 600 out of 4096 points are removed on average for being too closed to other points with a voxel size of 0.01. We also visualize the sparse voxel representation in Fig. 4. As the smallest independent semantic unit in the complex scene, the pedestrian is still recognizable, which means that we can ignore the quantization loss introduced by voxelization to some extent.

Inspired by Minkloc3D[18], we apply a very shallow

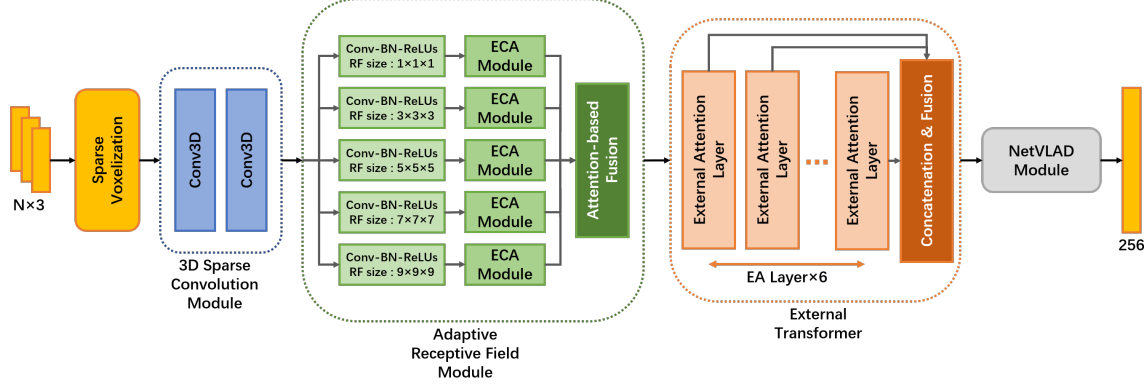


Figure 2. TransLoc3D Network Architecture. Our proposed TransLoc3D consists of four modules stacked in serial, including 3D Sparse Convolution Module, Adaptive Receptive Field Module (ARFM), External Transformer and a NetVLAD layer. ARFM is capable of adaptively adjusting the size of receptive field according to the input point cloud.

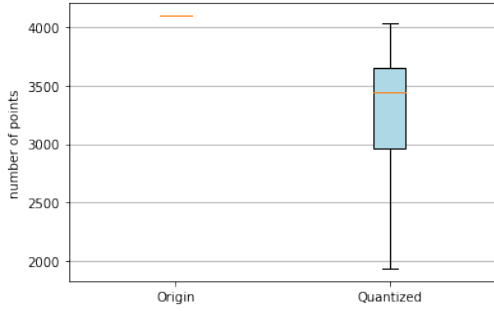


Figure 3. Change in the number of points. The distribution of original point number is shown as a box plot on the left, while the distribution of point number after quantization is shown on the right.

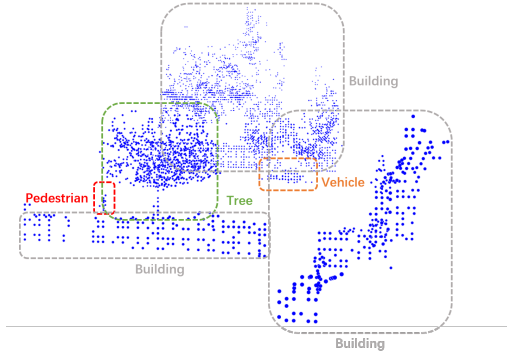


Figure 4. Visualization of sparse quantized point clouds. Various objects in the scene is denoted with dotted boxes of different colors.

network containing only two convolutional layers to aggregate local structure information. The details of the 3D sparse convolution module is illustrated in Tab. 1, where $\mathbb{C}_{a_k b_s}^c$ denotes a convolutional layer with c kernels of shape

$a \times a \times a$ and stride b . Same as Minkloc3D [18], the first convolution has a $5 \times 5 \times 5$ kernel to aggregate information from a larger area. In order to extract low-level geometric features, only one $2 \times 2 \times 2$ convolution with stride 2 is used in our network, which halves the spatial resolution. All convolutions are followed by a batch normalization [16] layer and a non-linear activation function.

3.2. Adaptive Receptive Field Module

NDT-Transformer [57] is the first Transformer-based network regarding to the place recognition task, in which the network learns a global descriptor from a set of 3D NDT cells. But intuitively, the fixed receptive field of each NDT cell is not well suited to the complex outdoor scenes. As shown in Fig. 4, there exists large size differences among objects in the scene, and our intuition is to employ networks with small receptive fields to learn representations for small objects such as pedestrians and vehicles, and those with large receptive fields for large objects like buildings, in order to capture clean and complete structure information.

The design of our proposed Adaptive Receptive Field Module (ARFM) is inspired by Selective Kernel Convolution (SK-Conv) [20], which is capable of adaptively aggregating information from neighborhoods of different sizes. We further improve the design by incorporating Efficient Channel Attention [48] mechanism. Unlike SK-Conv, we replace the dilated convolutions [4] with conventional convolutions because the combination of dilated convolution and sparse feature maps is demonstrated to have significant degradation in our experiments. More details of dilated convolution are presented in Sec. 4.4. Specifically, for the given feature map $X \in \mathbb{R}^{H \times W \times D \times C}$ output by the 3D sparse convolution module, we first conduct transformations $\mathcal{F}_i : X \rightarrow X'_i \in \mathbb{R}^{H \times W \times D \times C}$ with different receptive field sizes. Fig. 5 illustrates that ARFM consists of

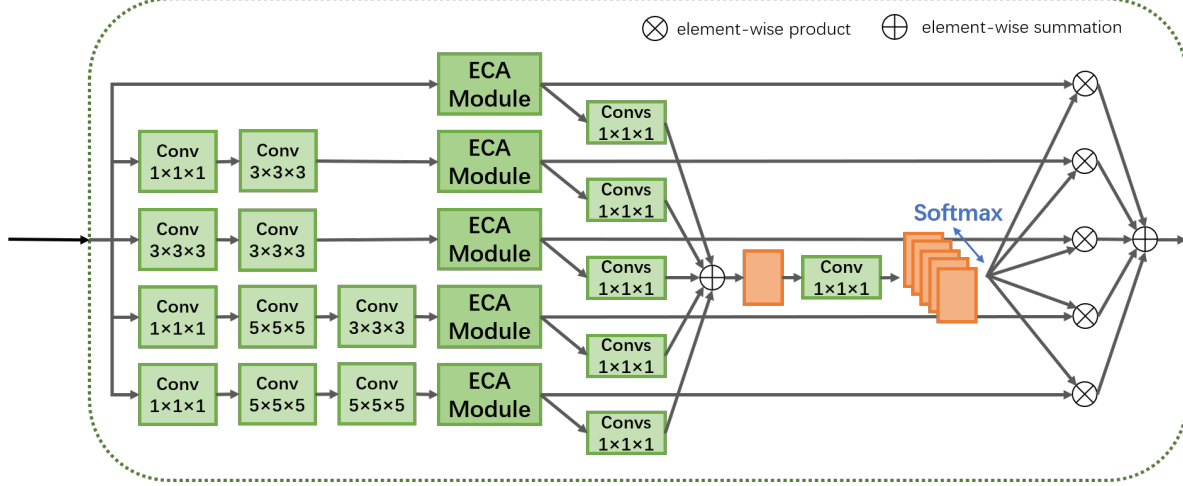


Figure 5. Adaptive Receptive Field Module. Information from neighborhoods of different sizes is aggregated on each branch, and then fed to ECA modules for further enhancement. Attention-based fusion mechanism is adopted to fuse information from different branches.

five paralleled branches, the receptive field sizes of which are $1 \times 1 \times 1$, $3 \times 3 \times 3$, $5 \times 5 \times 5$, $7 \times 7 \times 7$ and $9 \times 9 \times 9$ respectively. For computing efficiency, branches with receptive field sizes larger than $5 \times 5 \times 5$ is implemented by stacking multiple convolutions with kernel size $3 \times 3 \times 3$ and $5 \times 5 \times 5$. All convolutions are followed by a batch normalization [16] layer and ReLU, except for the last one in each branch.

Considering that pedestrians and vehicles make no contribution to place recognition, we incorporate an ECA [48] module in the ARFM to aggregate global information so that noisy features can be filtered out by channel attention. Formally, for the i -th branch, given the feature map $X'_i \in \mathbb{R}^{H \times W \times D \times C}$, we multiply features $x'_i \in \mathbb{R}^C$ in different positions by the same channel-wise weighting vector $w' \in \mathbb{R}^C$

$$x''_i = x'_i \otimes w' \quad (1)$$

$$w' = \sigma(\phi(\text{AvgPool}(X'_i))) \quad (2)$$

where σ denotes Sigmoid function, \otimes denotes element-wise product and ϕ indicates a linear mapping from the global descriptor to a shared weighting vector. In the last step of ARFM, the information originated from multiple branches are fused together by the gate mechanism

$$U = \sum_i W''_i \otimes X''_i \quad (3)$$

where $W''_i \in \mathbb{R}^{H \times W \times D \times C}$ denotes the attention weighting map of the i -th branch. As illustrated in Fig. 5, to obtain the weighting maps W''_i , we fuse results from multiple branches via element-wise summation first.

$$S = \sum_i \delta_i(X''_i) \quad (4)$$

Here δ_i is defined as a non-linear mapping function on the i -th branch. Notably, Selective Kernel Convolution [20] shrinks $S \in \mathbb{R}^{H \times W \times D \times C}$ through spatial dimensions $H \times W \times D$ for higher efficiency while we keep the spatial dimensions because global information has been aggregated by the ECA module. Therefore the i -th weighting map W_i is defined as

$$W''_i = \frac{\exp(\varphi_i(S))}{\sum_j \exp(\varphi_j(S))} \quad (5)$$

where φ_i denotes an element-wise non-linear mapping from aggregated information to the weighting maps of the i -th branch. It's implemented by a convolution with C kernels of shape $1 \times 1 \times 1$, followed by batch normalization.

3.3. External Transformer

Vanilla neural network enlarges the receptive field by stacking convolutional layers and pooling layers, which is adverse to extract low-level geometric information in our opinion. Inspired by ViT[8], the first Transformer-based architecture in computer vision, we aggregate the contextual information for one local descriptor from all other local descriptors using a Transformer-based module. Transformers [47] are models capable of drawing global dependencies via the self-attention mechanism, which makes global receptive field available to each neuron and efficiently enhances local features. As shown in Fig. 2, our proposed Transformer module includes 6 attention layers stacked in serial, as well as a shared non-linear mapping stacks at the head. The vanilla self-attention mechanism with multi-head attention is defined as

$$\text{Attn}(Q_i, K_i, V_i) = \text{Softmax}\left(\frac{Q_i K_i^T}{\sqrt{d_k}}\right) V_i \quad (6)$$

where d_k is the dimension of query features and Q_i, K_i, V_i denote the i -th head of queries, keys and values. However, the time and space complexity of computing attention weighting map is $O(N^2)$, where N indices the number of features fed to the self-attention layer. The mechanism limits the batch size in training process, therefore we use External Attention (EA) [11] to build our transformer architecture instead

$$\text{EA}(Q_i, K_i^{(M)}, V_i^{(M)}) = \text{Softmax}\left(\frac{Q_i K_i^{(M)T}}{\sqrt{d_k}}\right) V_i^{(M)} \quad (7)$$

$$(8)$$

where $K_i^{(M)}, V_i^{(M)} \in \mathbb{R}^{S \times d}$ denotes the i -th head of two external learnable memory units and the hyper-parameter S is the number of keys and values in EA mechanism. For further reduction of model parameters, the values $V_i^{(M)}$ are obtained by applying a linear mapping ϕ to the keys $K_i^{(M)}$ instead of an extra memory unit

$$V_i^{(M)} = \phi(K_i^{(M)}) \quad (9)$$

The space complexity of External Attention [11] is $O(N \times S)$, thus we can control the amount of memory consumed in training process by adjusting the hyper-parameter S . Same as PCT[10], we incorporate an offset-attention module with slight modification¹ to External Attention layer for further enhancement

$$F_{\text{out}} = \text{LBR}(F_{\text{EA}} - F_{\text{in}}) + F_{\text{in}} \quad (10)$$

$$F_{\text{EA}} = [\text{EA}(Q_i, K_i^{(M)}, V_i^{(M)})]$$

$$= [\text{Softmax}(Q_i K_i^{(M)T}) V_i^{(M)}] \quad (11)$$

Here LBR combines *Linear*, *BatchNorm* and *ReLU* layers, $F_{\text{in}}, F_{\text{out}}$ are the input and output features of EA module and $[\cdot]$ denotes the concatenation operation. Finally the output of each EA layer is concatenated by the feature dimension, followed by a transformation to aggregate information from different levels.

3.4. NetVLAD module

In this section, we aim to produce a discriminative global descriptor by aggregating the local features. Instead of General Mean pooling layer [37] used in Minkloc3D[18], we adopt a NetVLAD [1] layer following previous works operating on unordered point set representation for its stronger representational power. NetVLAD learns K cluster centers and sums the difference between the local descriptors and the corresponding cluster centers, to obtain a permutation-invariant descriptor. To make a fair comparison, NetVLAD

¹We replace $F_{\text{in}} - F_{\text{EA}}$ proposed in PCT[10] with $F_{\text{EA}} - F_{\text{in}}$, which has no effect on the representational ability of the model in theory, but has a slight improvement in our experiments.

is followed by a Multi-Layer Perceptron(MLP) to produce a global descriptor of the same size as that of previous state-of-the-arts.

3.5. Network training

Although a number of sophisticated loss functions have been proposed in deep metric learning, recent works [32, 39] show that their advantages over the classical triplet margin loss [14] is moderate. We use triplet margin loss to train our network, which requires an anchor, a positive example (structurally similar to the anchor) and a negative example (structurally dissimilar to the anchor):

$$\mathcal{L}_{\text{triplet}} = \frac{1}{N} \sum_{i=1}^N [||\delta_a - \delta_p||_2 - ||\delta_a - \delta_n||_2 + \alpha]_+ \quad (12)$$

Here δ_a, δ_p and δ_n denote the global descriptor of the anchor, positive and negative point cloud respectively. $[\cdot]_+$ denotes the loss function $\max(\cdot, 0)$ and α is the constant margin. Following Minkloc3D [18], at the beginning of each epoch the training set is partitioned into batches by randomly sampling positive pairs from the remaining data repeatedly. For each batch we compute two $n \times n$ binary masks indicating the structural similarity between each two point clouds. The discriminative descriptors of each point cloud in a batch is obtained by our proposed network. Then we construct informative triplets via batch hard mining approach [30] using two binary masks.

At the early stage of training, the model cannot produce sufficiently discriminative descriptors and mode collapse is more likely to occur with a large batch size. Therefore, we adaptively adjust the batch size as the training continues, as is proposed in Minkloc3D [18]. If the average number of triplets which produce non-zero loss accounts for over η of the total number, the batch size will be enlarged to α times of the previous value. Here α is a hyper-parameter larger than 1.

4. Experiments

4.1. Datasets

Following previous works[46, 55, 27, 18, 19] in place recognition, we use a modified Oxford RobotCar dataset [28] and three in-house datasets, including Business District(B.D.), Residual Area(R.A.) and University Sector(U.S.) to evaluate our method. Point clouds in Oxford RobotCar dataset are obtained by a Sick LMS-151 2D LiDAR scanner mounted on a moving vehicle, while others are obtained from Velodyne-64 LiDAR scanner. In order to collect data in all weather conditions, the vehicle traversed a route through central Oxford twice a week on average for over a year. The places are sampled with a fixed interval on the continuous trajectory of the vehicle, and the corresponding point clouds are generated by dividing the global

map into a set of submaps. During training, point cloud pairs with a distance less than 10m are defined as positive pairs, while more than 50m defined as negative pairs. The rest of point cloud pairs are neither positive nor negative. To better learn geometric features, all point clouds are pre-processed with the same pipeline. First the non-informative ground are removed from data, then the number of points is uniformly downsampled to 4096. Coordinates of each point are shifted and scaled to $[-1, 1]$.

4.2. Implementation Details

In order to improve the generalization ability of network and reduce the risk of overfitting, data augmentation is adopted to the preprocessing stage. Specifically, the preprocessing includes random jittering with a noise sampled from the normal distribution $\mathcal{N}(0, 0.001)$ and clipped to $[-0.002, 0.002]$, random translation with a vector sampled from the uniform distribution $[-0.01, 0.01]^3$, random point removal with the probability of $d_r \sim [0.0, 0.1]$, random symmetrical transformation and random rotation. We also use random fronto-parallel cuboid erasing approach proposed in [18] for further augmentation.

Augmented point clouds are quantized with quantization step 0.01, and then fed to 3D sparse convolutional module implemented by Minkowski Engine [5], an auto-differentiation library operated on sparse tensors. In our opinion, as the neural network deepens, the feature maps capture more high-level semantic information rather than local geometric information. Therefore, in order to focus on the output of the first few EA[11] layers, the hyperparameter S of each EA layer is set to 256, 128, 128, 64, 64, 64 in sequence. The number of heads is set to 2. The concatenation of outputs from different attention layers is transformed to 512-dimensional space, and then fed to NetVLAD[1]. With regard to the hyperparameters within NetVLAD, the size of the cluster is set to 64 and the dimensions of the output is set to 256 for fair comparisons. We also incorporate context gating mechanism[31], which was initially proposed for large-scale video understanding, into NetVLAD to produce more informative descriptors.

We adopt Adam optimizer with an initial learning rate $2e - 4$, and multiplied by 0.1 on epoch 80, 120 and 160. Same as Minkloc3D[18], the batch size is initially set to 32 and increased by 40% once the number of active triplets is less than 70% of the total. All experiments are conducted on a server with 6 NVidia GeForce GTX 1080Ti GPUs and a Intel i7-6850K CPU. The total GPU memory consumed in training process is 65.5 GB.

4.3. Comparisons

For a fair comparison, we follow the same evaluation protocol used in [46, 55, 27, 18, 19], in which case the Recall indices are used to measure the performance of net-

Network	Oxford	B.D.	R.A.	U.S.
PointNetVLAD[46]	80.3	65.3	60.3	72.6
PCAN[55]	83.8	66.8	71.2	79.1
DAGC[41]	87.5	71.2	75.7	83.5
LPD-Net[27]	94.9	89.1	90.5	96.0
SOE-Net[53]	96.4	88.5	91.5	93.2
Minkloc3D[18]	97.9	88.5	91.2	95.0
NDT-Transformer[57]	97.7	-	-	-
Minkloc++[19]	98.2	82.7	85.1	93.0
TransLoc3D(ours)	98.5	88.4	91.5	94.9

Table 2. Evaluation Results($AR@1\%$). Place recognition methods are trained on Oxford RobotCar dataset and evaluated on all the out-door and in-house datasets. Our method surpasses prior state-of-the-art on Oxford RobotCar dataset, and has a competitive generalization ability from out-door data to in-house data.

works. In addition to $AR@1$ (Average Recall at top 1), $AR@1\%$ is also used as a common evaluation metric, where the value of N is equal to 1% of the database size.

We compare our model with PointNetVLAD [46], PCAN[55], DAGC[41], LPD-Net[27] and the state-of-the-art methods including SOE-Net[53], Minkloc3D[18], Minkloc++[19], and NDT-Transformer[57]. All these models are trained on modified Oxford RobotCar dataset, and produce global descriptors of size 256. To verify the generalization ability of the methods, we also evaluate them on three in-house datasets without training on them. It’s worth noting that Minkloc++ is a multimodal architecture using late fusion to fuse geometric information from RGB images and 3D point clouds. For a fair comparison, we only use the 3D modality sub-branch of Minkloc++ to produce unimodal, point cloud based descriptors. The evaluation results are illustrated in Tab. 2. The performance of Minloc++ and NDT-Transformer on in-house datasets are not reported in their paper, thus we run the evaluation by ourselves if the source code or pretrained model is available. Otherwise we take the results reported by other works following the same evaluation protocol. It’s observed that our proposed TransLoc3D achieves state-of-the-art results on Oxford RobotCar dataset, with a 0.3 p.p. higher average recall@1% than the runner-up method, Minkloc++. Although the improvement of $AR@1\%$ seems to be moderate, remarkably, there’s almost no space from improvement in the metric $AR@1\%$. Compared with NDT-Transformer which is also based on a Transformer architecture, our method adopts a nearly cost-free preprocessing step and achieves a remarkable improvement of 0.8 p.p on average recall@1%, which illustrated the significance of ARFM. For indoor datasets, our model surpasses other models on R.A. dataset while slightly worse than LPD-Net on other datasets. This is because there exist huge differences in data distribution and LPD-Net takes hand-crafted

Network	AR@1	AR@1%
PointNetVLAD[46]	63.3	80.3
PCAN[55]	70.7	83.8
DAGC[41]	73.3	87.5
LPD-Net[27]	86.3	94.9
SOE-Net[53]	89.4	96.4
Minkloc3D[18]	93.8	97.9
NDT-Transformer[57]	93.8	97.7
Minkloc++[19]	93.9	98.2
TransLoc3D(ours)	95.0	98.5

Table 3. Evaluation Results on Oxford RobotCar dataset. Place recognition methods are both trained and evaluated on Oxford RobotCar dataset. Our method has a remarkable improvement of 1.1 p.p. on AR@1

features as input, which improves the generalization ability of the network by introducing prior knowledge. The following experiment shows that our method surpasses LPD-Net after finetuning.

To further demonstrate the capability of our model, we also compare various methods on Oxford RobotCar dataset using average recall@1. As illustrated in Tab. 3, our method is obviously better than previous state-of-the-art model, with an improvement of 1.1 p.p., which means that TransLoc3D has a significantly stronger discrimination ability than other methods.

Following PointNetVLAD[46], U.S. and R.A. are also added to the training data except for Oxford RobotCar dataset, in order to verify the generalization ability of models on unseen scenarios. Different from fusing outdoor data and in-house data proposed in Minkloc3D[18], we pretrain our model on Oxford RobotCar dataset, and then finetune the model with a small learning rate on in-house datasets. Tab. 4 illustrates evaluation results of various methods, where the evaluation of Minkloc++[19] is conducted by ourselves due to the lack of reported results, other results are reported by their authors. It’s obvious that our method is superior to previous methods. Notably, compared with the runner-up method performance on B.D. dataset, TransLoc3D achieves an improvement of 0.8 p.p. on average recall@1 and an improvement of 0.7 p.p. on average recall@1%. The result fully demonstrates the potential of our network on unseen datasets. The comparison to LPD-Net[27] shows that hand-crafted features contribute greatly to the model performance on condition that the amount of data is relatively small or there exist huge differences in the data. Otherwise, learning-based models have a stronger ability of extracting local geometric information.

4.4. Ablation Studies

We conduct ablation studies to evaluate the impact of different proposed components to the discrimination ability



Figure 6. Visualization of dilated convolution and conventional convolution on sparse feature map. Green cubes indicate all positions of non-zero values in sparse feature map, while red crosses indicate the receptive field of the center cube. Dilated convolution (on the left) cannot aggregate information from the neighborhood of the center cube.

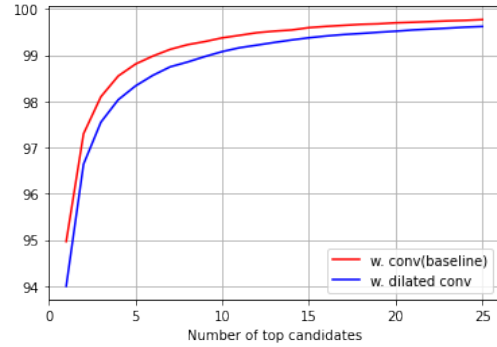


Figure 7. Ablation study on dilated convolution. Dilated convolution is not suitable for sparse feature maps.

of our method. In all experiments of this section, the network is trained and evaluated only using the Oxford RobotCar dataset. We first eliminate several independent modules including Adaptive Receptive Field Module, Efficient Channel Attention[48] and Attention-based Fusion Mechanism, referred as “w.o. ARFM”, “w.o. ECA” and “w.o. Attention-based Fusion”. We refer the complete network architecture as “baseline” in comparison. The elimination of Attention-based Fusion Mechanism is implemented by replacing weighted summation operator based on attention weights with a concatenation operator by the feature dimension, followed by a 1×1×1 convolution used to aggregate information from different branches. The results are illustrated in Tab.5. Compared with complete Transloc3D model, other models have a significant degradation on average recall@1, from 0.4 to 11.4 p.p., which demonstrated the importance of these modules.

Attention-based message aggregation mechanism from different receptive fields is first proposed in SK-Net[20], in which large receptive field branch is implemented by dilated convolution for further efficiency. However, dilated

Network	B.D.		R.A.		U.S.	
	$AR@1$	$AR@1\%$	$AR@1$	$AR@1\%$	$AR@1$	$AR@1\%$
PointNetVLAD[46]	80.1	86.5	82.7	93.1	86.1	90.1
PCAN[55]	80.3	87.0	82.3	92.3	83.7	94.1
DAGC[41]	81.3	88.5	82.8	93.4	86.3	94.3
LPD-Net[27]	90.8	94.4	90.8	96.4	94.4	98.9
SOE-Net[53]	89.0	92.6	90.2	95.9	91.8	97.7
Minkloc3D[18]	94.0	96.7	96.7	99.3	97.2	99.7
NDT-Transformer[57]	-	-	-	-	-	-
Minkloc++[19]	91.8	95.5	95.3	98.5	96.5	99.5
TransLoc3D(ours)	94.8	97.4	97.3	99.7	97.5	99.8

Table 4. Evaluation Results. Place recognition methods are trained on Oxford RobotCar, U.S. and R.A. dataset. We take results reported by authors and fill in the missing part with experiment results reported in Minkloc++[19]. After finetuning, our method archives state-of-the-art performance on all datasets

Network	$AR@1$	$AR@1\%$
w.o. ARFM	83.6	93.9
w.o. ECA	94.5	98.4
w.o. Attention-based Fusion	94.6	98.5
baseline	95.0	98.5

Table 5. Ablation study on various modules. The elimination of each module leads to a significant degradation on the performance.

convolution is not well suitable for sparse feature maps. Dilated convolution is implemented by sampling the input features from its receptive field with a fix stride larger than 1, which has been proved available in dense feature maps. This is because dense feature maps are capable of back-propagation anywhere and in most cases features distributed closely have a similarity in value, which we call local continuity of feature maps. On the contrary, sparse feature maps do not hold these properties. For computational efficiency, the positions of non-zero features in sparse feature maps do not change when adopting sparse convolution, which weakens local continuity of sparse feature maps. Moreover, for point cloud data, most non-zero features are distributed along the outer surface of objects. As illustrated in 6, the number of non-zero features fed to dilated convolutional layer is lower than the theoretical maximum, which leads to incomplete geometric information. Fig. 7 shows the comparison between ARFMs built on conventional convolutions and dilated convolutions. It can be seen that dilated convolution-based network has obvious degradation on average recall@N, which demonstrates that dilated convolution used in sparse feature maps has a obviously negative impact on performance compared with dense feature maps.

We also conduct an experiment on the influence of the number of branches in ARFM and the number of attention layers in Transformer. As illustrated in Fig.8, as the number of branches increases, the discrimination ability of descriptors produced by TransLoc3D becomes stronger, and

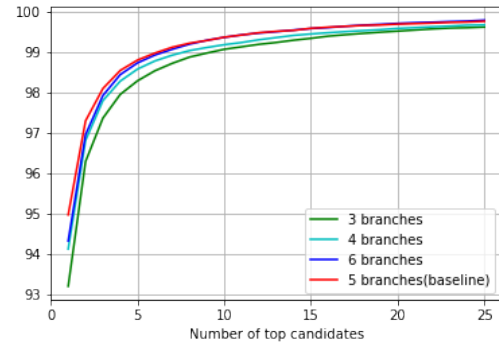


Figure 8. Ablation study on the number of branches in Adaptive Receptive Field Module. As the number of branches increases, average recall rises to saturation with 5 branches.

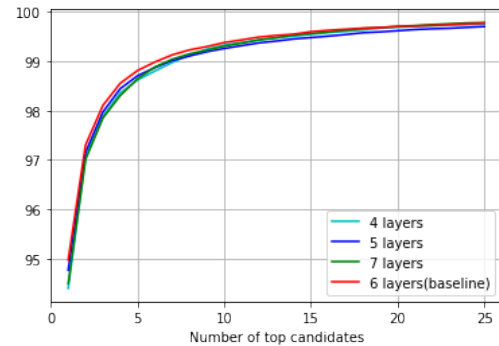


Figure 9. Ablation study on the number of attention layers in Transformer. Average Recall curves change slightly as the number of attention layers increases, indicating that TransLoc3D is not sensitive to the number of attention layers.

saturation occurs when using more than 5 branches, then average recall goes down. The result indicates that the local feature extractor requires aggregating geometric information from a local area larger than a certain thresh-

old to produce sufficiently discriminative descriptors fed to Transformers, while oversized receptive fields lead to too complicated geometric information for local descriptors to precisely represent. Fig.9 shows the performance of each model with a different number of layers. It can be observed that TransLoc3D with 6 layers only has a slightly improvement compared with others, which demonstrates the robustness of TransLoc3D to hyper-parameter selection.

5. Conclusion

In this paper, we emphasize the influence of size difference for objects in complex scenes, and propose a novel module named Adaptive Receptive Field Module to tackle this problem. We also introduce a novel network architecture named TransLoc3D built on Transformer and ARFM for place recognition. Extensive experiments show that our network achieves state-of-the-art performance on benchmark datasets and is robust to hyperparameter selection. We believe our work can promote further exploitation in visual transformer by showing its dependency on multi-scale geometric information.

Notably, there is nearly no room ($AR@1\%$ 98.5) for further improvement on Oxford RobotCar dataset. Larger datasets are required for place recognition, and light-weight models deserve more attention rather than time-consuming preprocessing operations. Future works include applying adaptive receptive fields on other tasks including object detection and semantic segmentation.

References

- [1] Relja Arandjelovic, Petr Gronát, Akihiko Torii, Tomás Padilla, and Josef Sivic. Netvlad: CNN architecture for weakly supervised place recognition. In *2016 IEEE Conference on Computer Vision and Pattern Recognition, CVPR 2016, Las Vegas, NV, USA, June 27-30, 2016*, pages 5297–5307. IEEE Computer Society, 2016. 2, 3, 6, 7
- [2] Peter W. Battaglia, Jessica B. Hamrick, Victor Bapst, Alvaro Sanchez-Gonzalez, Vinícius Flores Zambaldi, Mateusz Malinowski, Andrea Tacchetti, David Raposo, Adam Santoro, Ryan Faulkner, Çağlar Gülçehre, H. Francis Song, Andrew J. Ballard, Justin Gilmer, George E. Dahl, Ashish Vaswani, Kelsey R. Allen, Charles Nash, Victoria Langston, Chris Dyer, Nicolas Heess, Daan Wierstra, Pushmeet Kohli, Matthew Botvinick, Oriol Vinyals, Yujia Li, and Razvan Pascanu. Relational inductive biases, deep learning, and graph networks. *CoRR*, abs/1806.01261, 2018. 2
- [3] Nicolas Carion, Francisco Massa, Gabriel Synnaeve, Nicolas Usunier, Alexander Kirillov, and Sergey Zagoruyko. End-to-end object detection with transformers. In Andrea Vedaldi, Horst Bischof, Thomas Brox, and Jan-Michael Frahm, editors, *Computer Vision - ECCV 2020 - 16th European Conference, Glasgow, UK, August 23-28, 2020, Proceedings, Part I*, volume 12346 of *Lecture Notes in Computer Science*, pages 213–229. Springer, 2020. 3
- [4] Liang-Chieh Chen, George Papandreou, Iasonas Kokkinos, Kevin Murphy, and Alan L. Yuille. Deeplab: Semantic image segmentation with deep convolutional nets, atrous convolution, and fully connected crfs. *IEEE Trans. Pattern Anal. Mach. Intell.*, 40(4):834–848, 2018. 4
- [5] Christopher B. Choy, JunYoung Gwak, and Silvio Savarese. 4d spatio-temporal convnets: Minkowski convolutional neural networks. In *IEEE Conference on Computer Vision and Pattern Recognition, CVPR 2019, Long Beach, CA, USA, June 16-20, 2019*, pages 3075–3084. Computer Vision Foundation / IEEE, 2019. 7
- [6] Konrad P. Cop, Paulo V. K. Borges, and Renaud Dubé. Delight: An efficient descriptor for global localisation using lidar intensities. In *2018 IEEE International Conference on Robotics and Automation, ICRA 2018, Brisbane, Australia, May 21-25, 2018*, pages 3653–3660. IEEE, 2018. 2
- [7] Zhigang Dai, Bolun Cai, Yugeng Lin, and Junying Chen. UP-DETR: unsupervised pre-training for object detection with transformers. *CoRR*, abs/2011.09094, 2020. 3
- [8] Alexey Dosovitskiy, Lucas Beyer, Alexander Kolesnikov, Dirk Weissenborn, Xiaohua Zhai, Thomas Unterthiner, Mostafa Dehghani, Matthias Minderer, Georg Heigold, Sylvain Gelly, Jakob Uszkoreit, and Neil Houlsby. An image is worth 16x16 words: Transformers for image recognition at scale. *CoRR*, abs/2010.11929, 2020. 3, 5
- [9] Zhengyang Geng, Meng-Hao Guo, Hongxu Chen, Xia Li, Ke Wei, and Zhouchen Lin. Is attention better than matrix decomposition? In *International Conference on Learning Representations*, 2021. 3
- [10] Meng-Hao Guo, Junxiong Cai, Zheng-Ning Liu, Tai-Jiang Mu, Ralph R. Martin, and Shi-Min Hu. PCT: point cloud transformer. *Comput. Vis. Media*, 7(2):187–199, 2021. 6
- [11] Meng-Hao Guo, Zheng-Ning Liu, Tai-Jiang Mu, and Shi-Min Hu. Beyond self-attention: External attention using two linear layers for visual tasks. *CoRR*, abs/2105.02358, 2021. 3, 6, 7
- [12] Kai Han, An Xiao, Enhua Wu, Jianyuan Guo, Chunjing Xu, and Yunhe Wang. Transformer in transformer. *arXiv preprint arXiv:2103.00112*, 2021. 3
- [13] Li He, Xiaolong Wang, and Hong Zhang. M2DP: A novel 3d point cloud descriptor and its application in loop closure detection. In *2016 IEEE/RSJ International Conference on Intelligent Robots and Systems, IROS 2016, Daejeon, South Korea, October 9-14, 2016*, pages 231–237. IEEE, 2016. 2
- [14] Alexander Hermans, Lucas Beyer, and Bastian Leibe. In defense of the triplet loss for person re-identification. *CoRR*, abs/1703.07737, 2017. 3, 6
- [15] Qingyong Hu, Bo Yang, Linhai Xie, Stefano Rosa, Yulan Guo, Zhihua Wang, Niki Trigoni, and Andrew Markham. Randla-net: Efficient semantic segmentation of large-scale point clouds. In *2020 IEEE/CVF Conference on Computer Vision and Pattern Recognition, CVPR 2020, Seattle, WA, USA, June 13-19, 2020*, pages 11105–11114. IEEE, 2020. 2
- [16] Sergey Ioffe and Christian Szegedy. Batch normalization: Accelerating deep network training by reducing internal covariate shift. In Francis R. Bach and David M. Blei, editors, *Proceedings of the 32nd International Conference on Machine Learning, ICML 2015, Lille, France, 6-11 July 2015*,

- volume 37 of *JMLR Workshop and Conference Proceedings*, pages 448–456. JMLR.org, 2015. 4, 5
- [17] Giseop Kim and Ayoung Kim. Scan context: Egocentric spatial descriptor for place recognition within 3d point cloud map. In *2018 IEEE/RSJ International Conference on Intelligent Robots and Systems, IROS 2018, Madrid, Spain, October 1-5, 2018*, pages 4802–4809. IEEE, 2018. 2
- [18] Jacek Komorowski. Minkloc3d: Point cloud based large-scale place recognition. In *Proceedings of the IEEE/CVF Winter Conference on Applications of Computer Vision (WACV)*, pages 1790–1799, January 2021. 1, 2, 3, 4, 6, 7, 8, 9
- [19] Jacek Komorowski, Monika Wysoczanska, and Tomasz Trzcinski. Minkloc++: Lidar and monocular image fusion for place recognition. *CoRR*, abs/2104.05327, 2021. 2, 6, 7, 8, 9
- [20] Xiang Li, Wenhai Wang, Xiaolin Hu, and Jian Yang. Selective kernel networks. In *IEEE Conference on Computer Vision and Pattern Recognition, CVPR 2019, Long Beach, CA, USA, June 16-20, 2019*, pages 510–519. Computer Vision Foundation / IEEE, 2019. 2, 3, 4, 5, 8
- [21] Yunpeng Li, Noah Snavely, and Daniel P. Huttenlocher. Location recognition using prioritized feature matching. In Kostas Daniilidis, Petros Maragos, and Nikos Paragios, editors, *Computer Vision - ECCV 2010, 11th European Conference on Computer Vision, Heraklion, Crete, Greece, September 5-11, 2010, Proceedings, Part II*, volume 6312 of *Lecture Notes in Computer Science*, pages 791–804. Springer, 2010. 1
- [22] Tsung-Yi Lin, Piotr Dollár, Ross B. Girshick, Kaiming He, Bharath Hariharan, and Serge J. Belongie. Feature pyramid networks for object detection. In *2017 IEEE Conference on Computer Vision and Pattern Recognition, CVPR 2017, Honolulu, HI, USA, July 21-26, 2017*, pages 936–944. IEEE Computer Society, 2017. 2, 3
- [23] Liu Liu, Hongdong Li, and Yuchao Dai. Efficient global 2d-3d matching for camera localization in a large-scale 3d map. In *IEEE International Conference on Computer Vision, ICCV 2017, Venice, Italy, October 22-29, 2017*, pages 2391–2400. IEEE Computer Society, 2017. 1
- [24] Liu Liu, Hongdong Li, and Yuchao Dai. Stochastic attraction-repulsion embedding for large scale image localization. In *2019 IEEE/CVF International Conference on Computer Vision, ICCV 2019, Seoul, Korea (South), October 27 - November 2, 2019*, pages 2570–2579. IEEE, 2019. 1
- [25] Wei Liu, Dragomir Anguelov, Dumitru Erhan, Christian Szegedy, Scott E. Reed, Cheng-Yang Fu, and Alexander C. Berg. SSD: single shot multibox detector. In Bastian Leibe, Jiri Matas, Nicu Sebe, and Max Welling, editors, *Computer Vision - ECCV 2016 - 14th European Conference, Amsterdam, The Netherlands, October 11-14, 2016, Proceedings, Part I*, volume 9905 of *Lecture Notes in Computer Science*, pages 21–37. Springer, 2016. 3
- [26] Yongcheng Liu, Bin Fan, Shiming Xiang, and Chunhong Pan. Relation-shape convolutional neural network for point cloud analysis. In *IEEE Conference on Computer Vision and Pattern Recognition, CVPR 2019, Long Beach, CA, USA, June 16-20, 2019*, pages 8895–8904. Computer Vision Foundation / IEEE, 2019. 3
- [27] Zhe Liu, Shunbo Zhou, Chuanzhe Suo, Peng Yin, Wen Chen, Hesheng Wang, Haoang Li, and Yunhui Liu. Lpd-net: 3d point cloud learning for large-scale place recognition and environment analysis. In *2019 IEEE/CVF International Conference on Computer Vision, ICCV 2019, Seoul, Korea (South), October 27 - November 2, 2019*, pages 2831–2840. IEEE, 2019. 1, 2, 6, 7, 8, 9
- [28] Will Maddern, Geoff Pascoe, Chris Linegar, and Paul Newman. 1 Year, 1000km: The Oxford RobotCar Dataset. *The International Journal of Robotics Research (IJRR)*, 36(1):3–15, 2017. 3, 6
- [29] Martin Magnusson, Achim J. Lilienthal, and Tom Duckett. Scan registration for autonomous mining vehicles using 3d-ndt. *J. Field Robotics*, 24(10):803–827, 2007. 2, 3
- [30] R. Manmatha, Chao-Yuan Wu, Alexander J. Smola, and Philipp Krähenbühl. Sampling matters in deep embedding learning. In *IEEE International Conference on Computer Vision, ICCV 2017, Venice, Italy, October 22-29, 2017*, pages 2859–2867. IEEE Computer Society, 2017. 3, 6
- [31] Antoine Miech, Ivan Laptev, and Josef Sivic. Learnable pooling with context gating for video classification. *CoRR*, abs/1706.06905, 2017. 7
- [32] Kevin Musgrave, Serge J. Belongie, and Ser-Nam Lim. A metric learning reality check. In Andrea Vedaldi, Horst Bischof, Thomas Brox, and Jan-Michael Frahm, editors, *Computer Vision - ECCV 2020 - 16th European Conference, Glasgow, UK, August 23-28, 2020, Proceedings, Part XXV*, volume 12370 of *Lecture Notes in Computer Science*, pages 681–699. Springer, 2020. 6
- [33] JI Nelson and BJ Frost. Orientation-selective inhibition from beyond the classic visual receptive field. *Brain research*, 139(2):359–365, 1978. 3
- [34] Mark W Pettet and Charles D Gilbert. Dynamic changes in receptive-field size in cat primary visual cortex. *Proceedings of the National Academy of Sciences*, 89(17):8366–8370, 1992. 3
- [35] Charles Ruizhongtai Qi, Hao Su, Kaichun Mo, and Leonidas J. Guibas. Pointnet: Deep learning on point sets for 3d classification and segmentation. In *2017 IEEE Conference on Computer Vision and Pattern Recognition, CVPR 2017, Honolulu, HI, USA, July 21-26, 2017*, pages 77–85. IEEE Computer Society, 2017. 2, 3
- [36] Charles Ruizhongtai Qi, Li Yi, Hao Su, and Leonidas J. Guibas. Pointnet++: Deep hierarchical feature learning on point sets in a metric space. In Isabelle Guyon, Ulrike von Luxburg, Samy Bengio, Hanna M. Wallach, Rob Fergus, S. V. N. Vishwanathan, and Roman Garnett, editors, *Advances in Neural Information Processing Systems 30: Annual Conference on Neural Information Processing Systems 2017, December 4-9, 2017, Long Beach, CA, USA*, pages 5099–5108, 2017. 2, 3
- [37] Filip Radenovic, Giorgos Tolias, and Ondrej Chum. Fine-tuning CNN image retrieval with no human annotation. *IEEE Trans. Pattern Anal. Mach. Intell.*, 41(7):1655–1668, 2019. 2, 6

- [38] Joseph Redmon, Santosh Kumar Divvala, Ross B. Girshick, and Ali Farhadi. You only look once: Unified, real-time object detection. In *2016 IEEE Conference on Computer Vision and Pattern Recognition, CVPR 2016, Las Vegas, NV, USA, June 27-30, 2016*, pages 779–788. IEEE Computer Society, 2016. [2, 3, 5](#)
- [39] Karsten Roth, Timo Milbich, Samarth Sinha, Prateek Gupta, Björn Ommer, and Joseph Paul Cohen. Revisiting training strategies and generalization performance in deep metric learning. In *Proceedings of the 37th International Conference on Machine Learning, ICML 2020, 13-18 July 2020, Virtual Event*, volume 119 of *Proceedings of Machine Learning Research*, pages 8242–8252. PMLR, 2020. [6](#)
- [40] Michael P Sceniak, Dario L Ringach, Michael J Hawken, and Robert Shapley. Contrast’s effect on spatial summation by macaque v1 neurons. *Nature neuroscience*, 2(8):733–739, 1999. [3](#)
- [41] Qi Sun, Hongyan Liu, Jun He, Zhaoxin Fan, and Xiaoyong Du. DAGC: employing dual attention and graph convolution for point cloud based place recognition. In Cathal Gurin, Björn ör Jónsson, Noriko Kando, Klaus Schöffmann, Yi-Ping Phoebe Chen, and Noel E. O’Connor, editors, *Proceedings of the 2020 on International Conference on Multimedia Retrieval, ICMR 2020, Dublin, Ireland, June 8-11, 2020*, pages 224–232. ACM, 2020. [1, 2, 7, 8, 9](#)
- [42] Zhiqing Sun, Shengcao Cao, Yiming Yang, and Kris Kitani. Rethinking transformer-based set prediction for object detection. *CoRR*, abs/2011.10881, 2020. [3](#)
- [43] Christian Szegedy, Sergey Ioffe, Vincent Vanhoucke, and Alexander A. Alemi. Inception-v4, inception-resnet and the impact of residual connections on learning. In Sander P. Singh and Shaul Markovitch, editors, *Proceedings of the Thirty-First AAAI Conference on Artificial Intelligence, February 4-9, 2017, San Francisco, California, USA*, pages 4278–4284. AAAI Press, 2017. [3](#)
- [44] Christian Szegedy, Wei Liu, Yangqing Jia, Pierre Sermanet, Scott E. Reed, Dragomir Anguelov, Dumitru Erhan, Vincent Vanhoucke, and Andrew Rabinovich. Going deeper with convolutions. In *IEEE Conference on Computer Vision and Pattern Recognition, CVPR 2015, Boston, MA, USA, June 7-12, 2015*, pages 1–9. IEEE Computer Society, 2015. [3](#)
- [45] Christian Szegedy, Vincent Vanhoucke, Sergey Ioffe, Jonathon Shlens, and Zbigniew Wojna. Rethinking the inception architecture for computer vision. In *2016 IEEE Conference on Computer Vision and Pattern Recognition, CVPR 2016, Las Vegas, NV, USA, June 27-30, 2016*, pages 2818–2826. IEEE Computer Society, 2016. [3](#)
- [46] Mikaela Angelina Uy and Gim Hee Lee. Pointnetvlad: Deep point cloud based retrieval for large-scale place recognition. In *2018 IEEE Conference on Computer Vision and Pattern Recognition, CVPR 2018, Salt Lake City, UT, USA, June 18-22, 2018*, pages 4470–4479. IEEE Computer Society, 2018. [1, 2, 6, 7, 8, 9](#)
- [47] Ashish Vaswani, Noam Shazeer, Niki Parmar, Jakob Uszkoreit, Llion Jones, Aidan N. Gomez, Lukasz Kaiser, and Illia Polosukhin. Attention is all you need. In Isabelle Guyon, Ulrike von Luxburg, Samy Bengio, Hanna M. Wallach, Rob Fergus, S. V. N. Vishwanathan, and Roman Garnett, editors, *Advances in Neural Information Processing Systems 30: Annual Conference on Neural Information Processing Systems 2017, December 4-9, 2017, Long Beach, CA, USA*, pages 5998–6008, 2017. [2, 3, 5](#)
- [48] Qilong Wang, Banggu Wu, Pengfei Zhu, Peihua Li, Wangmeng Zuo, and Qinghua Hu. Eca-net: Efficient channel attention for deep convolutional neural networks. In *2020 IEEE/CVF Conference on Computer Vision and Pattern Recognition, CVPR 2020, Seattle, WA, USA, June 13-19, 2020*, pages 11531–11539. IEEE, 2020. [2, 4, 5, 8](#)
- [49] Wenhai Wang, Enze Xie, Xiang Li, Deng-Ping Fan, Kaitao Song, Ding Liang, Tong Lu, Ping Luo, and Ling Shao. Pyramid vision transformer: A versatile backbone for dense prediction without convolutions. *CoRR*, abs/2102.12122, 2021. [3](#)
- [50] Yue Wang, Yongbin Sun, Ziwei Liu, Sanjay E. Sarma, Michael M. Bronstein, and Justin M. Solomon. Dynamic graph CNN for learning on point clouds. *ACM Trans. Graph.*, 38(5):146:1–146:12, 2019. [2](#)
- [51] Yuqing Wang, Zhaoliang Xu, Xinlong Wang, Chunhua Shen, Baoshan Cheng, Hao Shen, and Huaxia Xia. End-to-end video instance segmentation with transformers. *CoRR*, abs/2011.14503, 2020. [3](#)
- [52] Zhirong Wu, Shuran Song, Aditya Khosla, Fisher Yu, Linguang Zhang, Xiaoou Tang, and Jianxiong Xiao. 3d shapenets: A deep representation for volumetric shapes. In *IEEE Conference on Computer Vision and Pattern Recognition, CVPR 2015, Boston, MA, USA, June 7-12, 2015*, pages 1912–1920. IEEE Computer Society, 2015. [3](#)
- [53] Yan Xia, Yusheng Xu, Shuang Li, Rui Wang, Juan Du, Daniel Cremers, and Uwe Stilla. Soe-net: A self-attention and orientation encoding network for point cloud based place recognition. *CoRR*, abs/2011.12430, 2020. [2, 7, 8, 9](#)
- [54] Zetong Yang, Yanan Sun, Shu Liu, and Jiaya Jia. 3dssd: Point-based 3d single stage object detector. In *2020 IEEE/CVF Conference on Computer Vision and Pattern Recognition, CVPR 2020, Seattle, WA, USA, June 13-19, 2020*, pages 11037–11045. IEEE, 2020. [2](#)
- [55] Wenxiao Zhang and Chunxia Xiao. PCAN: 3d attention map learning using contextual information for point cloud based retrieval. In *IEEE Conference on Computer Vision and Pattern Recognition, CVPR 2019, Long Beach, CA, USA, June 16-20, 2019*, pages 12436–12445. Computer Vision Foundation / IEEE, 2019. [1, 2, 6, 7, 8, 9](#)
- [56] Sixiao Zheng, Jiachen Lu, Hengshuang Zhao, Xiatian Zhu, Zekun Luo, Yabiao Wang, Yanwei Fu, Jianfeng Feng, Tao Xiang, Philip H. S. Torr, and Li Zhang. Rethinking semantic segmentation from a sequence-to-sequence perspective with transformers. *CoRR*, abs/2012.15840, 2020. [3](#)
- [57] Zhicheng Zhou, Cheng Zhao, Daniel Adolfsson, Songzhi Su, Yang Gao, Tom Duckett, and Li Sun. Ndt-transformer: Large-scale 3d point cloud localisation using the normal distribution transform representation. *CoRR*, abs/2103.12292, 2021. [1, 2, 3, 4, 7, 8, 9](#)